

7. IDENTIFICATION OF CLAY MINERALS AND ASSOCIATED MINERALS	227
Clay Mineral Identification—General Principles	228
Illite and Glauconite	233
Chlorite and Kaolinite	233
Vermiculite	239
Smectite	241
Sepiolite, Palygorskite, and Halloysite	243
060 Reflections	244
The Use of <i>hkl</i> Reflections for the Determination of Polytypes	246
Chlorite Polytypes	246
The Kaolin Polytypes	247
The Micas, Illite, and Glauconite	247
Nonclay Minerals	248
Silica Minerals	250
Feldspar	252
Zeolites	254
Carbonates	255
Apatite, Pyrite, and Jarosite	256
Gypsum, Anhydrite, Celestite, and Barite	257
Lepidocrocite, Goethite, Gibbsite, and Anatase	258
Summary	259
References	

Chapter 7

Identification of Clay Minerals and Associated Minerals

We have considered the structures and the chemical nature of clay minerals as well as their interaction with X-rays. Now we will focus on the process of gathering and using X-ray diffraction data for the identification and analysis of clay minerals, but we must be careful not to narrow our focus too much for three reasons. First, not all minerals in the clay-sized fraction are clay minerals. Second, there is almost always more to a rock sample than the clay-sized fraction. Third, X-ray diffraction, though extremely powerful, often must be supplemented by information from other analytical techniques.

There are two levels of analysis, qualitative and quantitative, and, depending on the time available and the nature of a project, there are different

levels of qualitative analysis. But if an analysis is going to be called quantitative, there is only one level and that is the very best that you can do, and even that will often not be good enough. It seems safe to assume that this text provides sufficient background for anyone who wants to do simple qualitative analysis of geologic materials consisting of several components. On the other hand, if quantitative analysis is achievable at all, it requires a great deal of experience, patience, luck, and skill. At present, quantitative analysis may be more of an art than a science.

The qualitative identification procedure begins by searching for a mineral that will explain the strongest peak or peaks, then confirming the choice by finding the positions of weaker peaks for the same mineral. Once a set of peaks is confirmed as belonging to a mineral, these peaks are eliminated from consideration. From the remaining peaks, again search for a mineral that will explain the strongest remaining peak or peaks and then confirm this by looking for its peaks of lesser intensity. Repeat until all peaks are identified. For example, though quartz is not a clay mineral, it is very often present in the clay-size fraction. Its strongest peak occurs at $26.65^\circ 2\theta$ for $\text{CuK}\alpha$. If this peak is present, then automatically check the $20.85^\circ 2\theta$ position, where the second-most-intense peak occurs. By using Table 7.8B you can locate the other peaks of quartz, all which then may be removed from consideration as you concentrate on the remaining peaks. Quartz can be more of a friend than a foe. Its peak positions are, for our purposes, invariant because the quartz structure tolerates no significant atomic substitutions. Thus the quartz pattern is a built-in internal standard against which you can estimate the accuracy and precision of peak positions for the other phases present. Precise measurements of d are required to measure the composition of mixed-layered minerals, and for the very best work you must add such a standard to your sample if quartz is not present. Errors in peak position arise mostly from the sample position errors mentioned in Chapters 2 (p. 44) and 9 (p. 299), and you often cannot minimize them to acceptable levels. The use of an internal standard is the best, and often the only, solution.

We encourage you to collect a set of X-ray diffraction tracings of the minerals you commonly encounter. Comparing tracings of unknowns against those of known minerals is an effective, quick, and accurate identification procedure. For example, Frondel (1962, p. 34) has a foldout of a diffraction tracing and table of spacings of quartz that you will find useful. Make your own at the conditions at which you normally run your machine.

CLAY MINERAL IDENTIFICATION—GENERAL PRINCIPLES

Clay minerals are identified by using X-ray diffraction patterns (diffractograms or diffraction tracings) of oriented aggregates that enhance the basal, or $00l$, reflections. hkl peaks are not very diagnostic because the

structures of most clay minerals are very similar in their X and Y directions. It is the atomic pattern along Z that is the most different from mineral to mineral. The JCPDS powder diffraction cards that are so useful for the identification of other minerals are useless or worse for clay minerals because they usually have been prepared from random orientations of the mineral powder; often what is listed as the strongest reflection for a clay mineral or mica will not even be visible on a pattern prepared from an oriented aggregate. Some of the newer cards, due to G. W. Brindley, are exceptions, and do indeed show the $00l$ diffraction profile for oriented aggregates. In addition, in the JCPDS 1993 edition of the *Mineral Powder Diffraction File Databook*, Appendix A shows $00l$ XRD tracings of common clay minerals. In this book, all diffraction pattern references for clay minerals apply to the $00l$ series unless otherwise specified, and $\text{CuK}\alpha$ radiation is assumed for all tables and calculated and experimental diffraction patterns.

The intent here is to provide a practical basis for the identification of the “simple” or noninterstratified clay minerals. The interstratified minerals are worth a chapter of their own, so methods for their identification are deferred to Chapter 8.

Clay mineral diffraction patterns contain a good deal of character. This character is manifested by the peak’s position, intensity, shape, and breadth. Peak position is determined by the Bragg law (Chapter 3), which is written as $n\lambda = 2d\sin\theta$. If the analysis is one dimensional, l may be substituted for n and the equation rearranged to give $l\lambda/2d = \sin\theta$. Now we have two constants, $d = d(001)$ and λ , and if θ is small, the angle may be substituted for its sine and we have a working result of $\theta = l \times (\text{constant})$. This equation means that at small diffraction angles the various members of the $00l$ series are equidistant. What are “small diffraction angles”? Well, most of the important clay peaks are at 2θ values of 40° or less; therefore, θ is 20° or less, and that value is sufficiently small to fit the foregoing argument to a pretty good approximation. Figure 7.1 shows the separation of the $00l$ series for chlorite, and you can see that the peaks are evenly spaced. In practice a ruler is unnecessary—simply holding your fingers at the proper fixed separation is good enough to identify the different reflections that belong to the same clay mineral.

Peak intensity was treated in Chapter 3. We simply remind you that relative $00l$ intensities are controlled by chemical composition and the positions of atoms in the unit cell, some characteristics of the sample, and the Soller slits on the goniometer.

Peak breadth for the $00l$ reflections from clay minerals is inversely proportional to the mean dimension (in \AA) normal to the diffracting planes in an optically coherent domain, i.e., the thinner the crystallites (= domain), the broader the peak. Recall that we discussed reasons for peak breadth in the text associated with Fig. 3.13, p. 85. By breadth, we mean the width of the diffraction maximum or peak at half its height above background (B in Fig.

3.12). Well-crystallized minerals such as quartz, for which domains are thousands of Ångstroms, produce sharp lines whose breadths depend only on the optical distortions inherent in the diffraction apparatus. But as domain size becomes smaller, noticeable line broadening occurs and is easily evident in diffraction patterns of clay minerals for which the optical domains are a few hundred Ångstroms or less in thickness. *The importance of line breadth for*

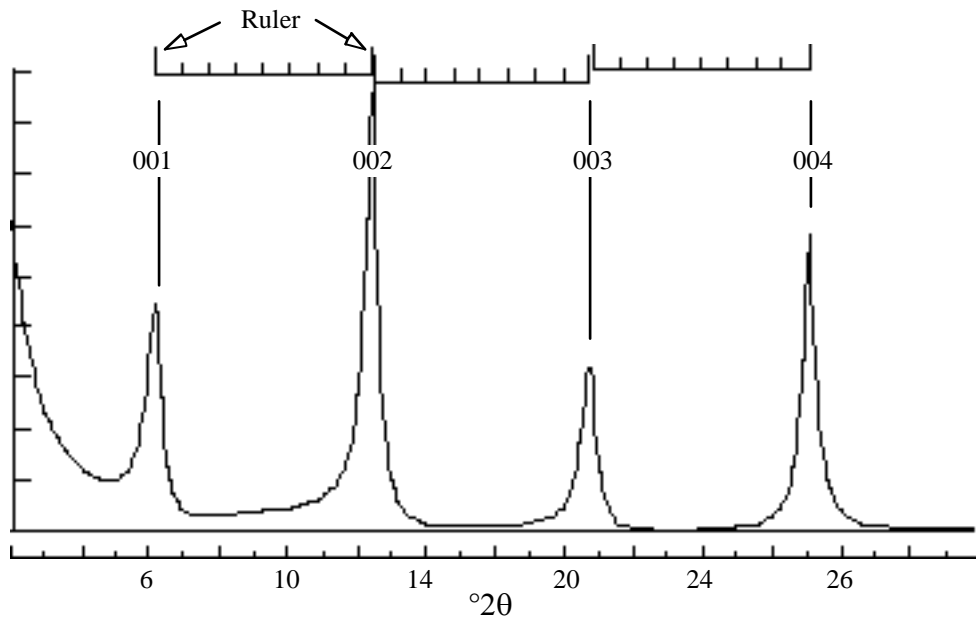


Fig. 7.1. Uniform separation of members of the 00*l* diffraction series for chlorite.

qualitative analysis is that it tells us at a glance which reflections are due to clay minerals and which might be assigned to other minerals, such as quartz, calcite, zeolites, pyrite, etc. In addition, all members of the 00*l* series from a given species have the same breadth (at low 2θ), so if your pattern contains broad (> 0.2 to 0.3°) lines, some of which are broader than others, the sample contains more than one clay mineral type. (We will deal with exceptions to this in the next chapter.) Figure 7.2 shows a pattern of a sample that contains thick crystallites of illite (sharp peaks), thin crystallites of kaolinite (broad peaks), and quartz (very sharp peaks). With no other knowledge, you should be able to conclude that the sample contains at least two clay minerals and one nonclay mineral. The rule of equidistant 00*l* peaks shows that the broad peaks belong to one series and the sharper peaks to another. You will, after you gain a bit of experience, also guess that the illite 003 reflection is superimposed on an intense peak of a nonclay mineral. This conclusion can be verified by a high-resolution scan plotted at an expanded horizontal scale that will produce, for the reflection near $26.6^\circ 2\theta$, a shape that can only be interpreted as the superposition of a sharp peak on a much broader one.

Identification of clay minerals can be accomplished by careful

consideration of peak positions and intensities, which are compared to published values in the literature. But with a little experience, you will not identify clay minerals this way. After all, the identification of clay minerals is a simple procedure, much simpler than the qualitative analyses of bulk rock powders that can contain many minerals, each of which has a complicated pattern that produces many interferences on the peaks of other minerals

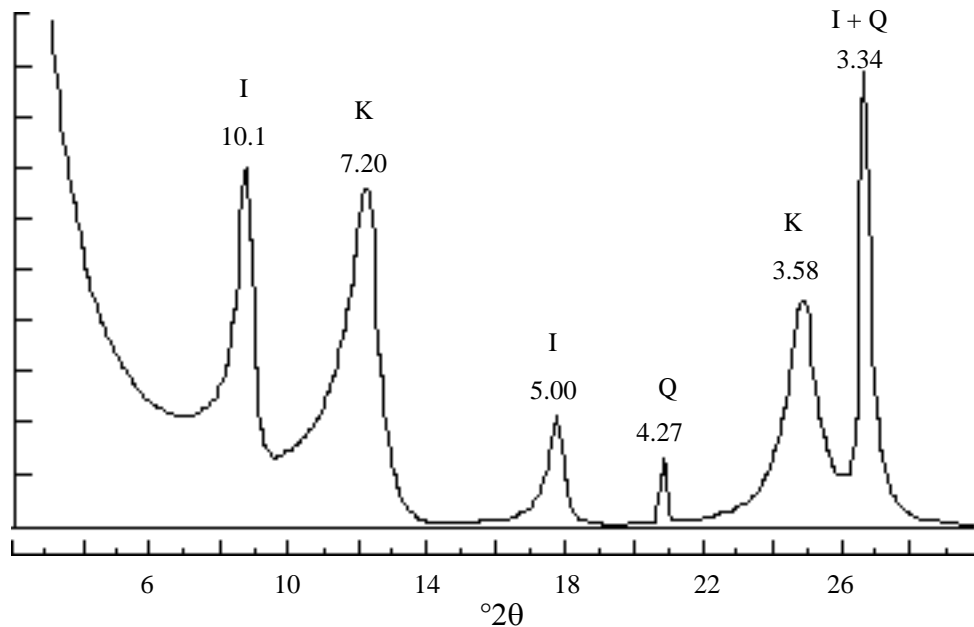


Fig. 7.2. A mixture of illite, kaolinite, and quartz.

present. The diffractionist will quickly grow familiar with the “image,” that is, the diffraction pattern, of a given clay mineral species and will recognize it in a diffractogram in much the same way that the face of a friend can be instantly recognized in a crowd. If a mixture is too complicated for that, the best way to proceed is to ask, “Is illite present?” Then, “Is vermiculite present?” “Is kaolinite present?” “Is chlorite present?” “Is smectite present?” If these questions can be answered, the analysis is complete, for with the exceptions of palygorskite, sepiolite, and the mixed-layered clay minerals, the interrogation has considered all the clay minerals likely to be found in sedimentary rocks, and if halloysite is included, the list covers soils as well. Some may regard this subjective procedure as “cheating.” But why do things the hard way? If you are a geologist and have collected the rocks yourself, or at least communicated with the person who did, then you know that the sample is a limestone or a shale or some other sedimentary rock type. Limestones probably do not contain olivine, nor is a sandstone likely to be rich in cuprite. Qualitative analysis contains elements of creative art. It is not entirely a science. One element is involved with interpreting the shapes, intensities, and positions of peaks, and another is the consideration of the

geological setting of the sample when interpreting the X-ray diffraction pattern.

For some samples, peaks will remain after others have been assigned to identified minerals. Then a second level of inquiry is needed to identify unfamiliar (or exotic) minerals. At that point, reference must be made to published data on the possibilities. In this category lie talc, pyrophyllite, paragonite, and the nonclay minerals that make up the aluminum and iron hydroxides and oxy-hydroxides, which may produce diffraction peaks that are broad like those of the clay minerals. Zeolites can be troublesome because they have reflections in the same low- 2θ range as the clay minerals, but they can usually be identified because their peaks are sharp and thus do not resemble clay mineral reflections. If you are reduced to identifying a completely unknown phase, first check the phases that match the peaks at the lowest diffraction angles. These are diagnostic because there are few phases with peaks in the very low-angle range. Check this out by examining the JCPDS index for inorganic phases. Not many minerals have reflections for which $d > 10 \text{ \AA}$, but many substances have peaks of $d = 2 \text{ \AA}$ or so. Chen's (1977) booklet listing the key peaks of minerals by 2θ and d can be helpful for pursuing the identity of unknowns.

These methods provide only a first step in qualitative analysis, because no consideration has been given to the speciation of the clay groups identified. For example, the word *smectite* covers a number of different smectites, each of which is given a name and has a defined range of composition (as in Table 4.3, p. 131). But for many applications a crude analysis is all that is required, and that can often be accomplished simply by inspection of the diffraction pattern.

Many identifications will be compromised by peak interferences that preclude or at least complicate the simple approach we have described. Then the material must be subjected to one or more chemical treatments (see Chapter 5) and reexamined by X-ray diffraction methods.

Let us now discuss the diffraction patterns of the various clay minerals, point out the common interferences, and suggest ways to deal with them. The diffraction patterns shown here have been calculated by computer methods and record correct relative intensities for each pattern. Absolute intensities have been adjusted to provide the scale most favorable for viewing the diagnostic features of each pattern. The relative intensities are correct only if the sample is thick enough and long enough (see Chapter 9). A 1° beam (divergence) slit is assumed in conjunction with a sample length of 4.6 cm, and this configuration causes weakening of peaks in the 5° to 6° 2θ region by about 50%. These conditions were selected because the 1° slit and such sample lengths are routine in most laboratories. We need not worry about the lowangle intensity distortion because it isn't very important for qualitative analysis, and the low-angle peaks are not suitable for quantitative analysis for reasons that are discussed in Chapter 9. For all calculations, a Lorentz-

polarization factor has been applied that is realistic for typical, well-oriented samples, analyzed using a diffractometer equipped with only one Soller slit (Reynolds, 1986). If your instrument uses two Soller slits, the intensities at high 2θ will be diminished somewhat, compared with the patterns shown here.

The X-ray diffraction patterns in Chapters 3 through 9 have been calculated by the computer program NEWMOD[©] (Reynolds, 1985), details of which are given in the Appendix. The program handles mixed-layered and simple clay minerals and takes into account diffractometer characteristics and setup. It provides adjustable chemical and structural parameters. With a few exceptions, we have elected to use calculated diffractograms because of the difficulties inherent in accumulating clay mineral standards that (1) have excellent diffraction characteristics, (2) are free from other mineral components that produce diffraction peak interferences, (3) have well-documented compositions and structures, and (4) are sufficiently diverse to illustrate the many examples required. Our approach is to show you many complete $00l$ diffraction patterns to provide the kind of experience necessary for the development of good analytical instincts; we don't think that tables of spacings and intensities accomplish that end. Finally, as you will see in Chapter 9, calculated diffraction patterns provide the best means of standardization for quantitative analysis and will be used for that purpose throughout our discussion. A disadvantage of calculated patterns may be that they "look too good" and don't provide you with an appreciation of the real world. A collection of your own diffractograms, therefore, is still an effective device for preliminary identification.

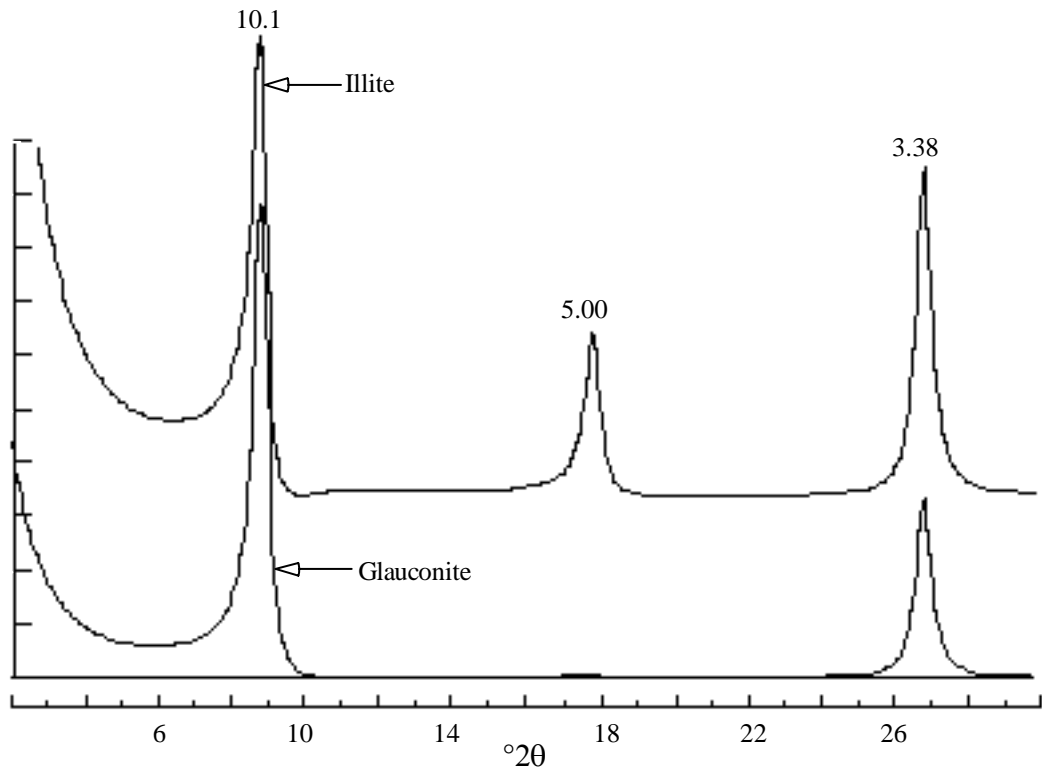


Fig. 7.3. Illite and glauconite.

Illite and Glauconite

Figure 7.3 shows patterns for pure illite and pure glauconite. The profiles are unaffected by ethylene glycol solvation and heating to 550°C and are difficult to confuse with those of any other clay mineral. Glauconite has a higher 001/003 intensity ratio than illite, but the main difference is the very weak or nonexistent glauconite 002 reflection whose weakness is caused by heavy scattering from octahedral iron. (See Fig. 3.10, p. 75 and related discussion. Can you adapt the problem associated with Fig. 3.10 to explain the difference in the 002 intensities in Fig. 7.3?) Diffractograms of the dioctahedral glauconite are difficult to distinguish from those of trioctahedral phlogopite and biotite unless the 060 reflection (see Table 7.4) can be measured to differentiate trioctahedral from dioctahedral minerals, but phlogopite-biotite minerals are rarely encountered in <2 μm size fractions of sedimentary rocks.

Chlorite and Kaolinite

Chlorite and kaolinite have very different structures and geological occurrences, but they are discussed together here because of the difficulties they present in mutual mixtures. Chlorite has a basal series of diffraction peaks based on a first-order reflection from a $d(001)$ of 14.2 Å, and kaolinite has reflections based on a 7.1 Å structure. Even-order chlorite peaks superimpose or nearly superimpose on the members of the kaolinite 001

series. High-Fe chlorites have weak odd-order reflections, so weak that the 001 peak is easily obscured or not noticed, so the distinction between chlorite and kaolinite is most difficult when Fe-rich chlorites are involved. Figure 7.4 illustrates the problem.

There are several methods for identifying these minerals in mixtures. Most kaolinites have the 002 peak at $24.9^\circ 2\theta$, and common chlorites have their 004 reflection at $\sim 25.1^\circ 2\theta$. The lines will be sharp if the crystallites are thick, and if they are, you can see resolution or partial resolution of the two. For some samples, evidence for both phases is suggested by a greater peak breadth at $25^\circ 2\theta$ than at $12.5^\circ 2\theta$. If large concentrations of both phases are present, the best method of identification is to look for the kaolinite 003 and the chlorite 003 peaks. Neither of these weak reflections is interfered with by reflections from the other mineral. The intensities of the 00*l* series can also be of help here. The intensity ratio for the kaolinite 002/003 is about 10. If the measured ratio is much greater than this, a significant contribution from the chlorite 004 is indicated for the peak at $25^\circ 2\theta$. Positive identification of chlorite is provided by peaks at 6.2 and $18.8^\circ 2\theta$, but these peaks are often weak and may not be detectable if the chlorite concentration is low or if its Fe content is high.

A difficulty arises when only weak reflections are present at 12.5 and $25^\circ 2\theta$. Such a sample could contain only chlorite, only kaolinite, or a mixture of the two. In this situation, the sample may be treated chemically or heated and then reexamined. Heating chlorite to 550°C for 1 h causes dehydroxylation of the hydroxide sheet with attendant changes in the diffraction pattern. The intensity of the 001 reflection usually increases greatly and shifts to about 6.3 to $6.4^\circ 2\theta$, and the 002, 003, and 004 reflections are much weakened (but not eliminated). At this temperature, kaolinite becomes amorphous to X-rays and its diffraction pattern disappears. This test may suggest that chlorite is present or that kaolinite is present and chlorite is absent. It will not give final and complete results for a sample that contains both kaolinite and chlorite. An additional treatment is required for dealing with such mixtures.

An aliquot of the sample should be boiled for 2 h in 1 N HCl. This step dissolves most chlorites, and any residual peaks at 12.5 and $25^\circ 2\theta$ indicate the presence of kaolinite. Mg-rich chlorites may be unaffected by this treatment, however, and though not common in sedimentary rocks, their possible presence always leaves some doubt about the results of an acid digestion.

There is a definitive method for identifying mixtures of kaolinite and chlorite, and only the difficulty of application makes it nonroutine. Kaolinite can be expanded by certain reagents that form strong hydrogen bonds (MacEwan and Wilson, 1980, p. 239). The expanded kaolinite produces a changed and recognizable diffraction pattern that is not interfered with by

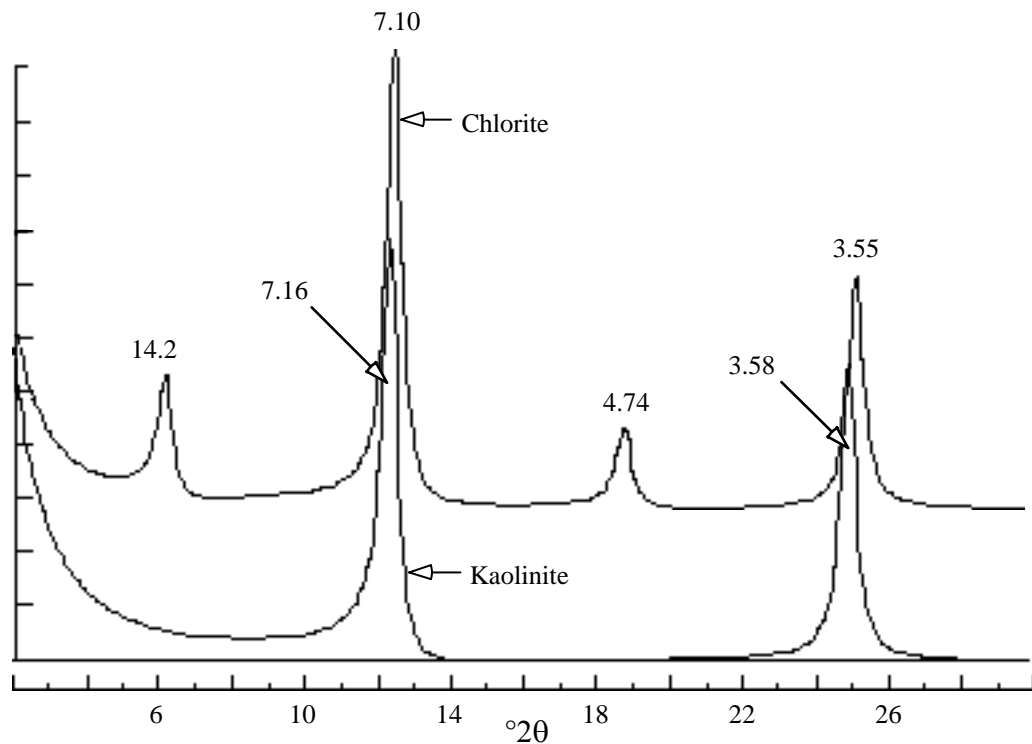


Fig. 7.4. Kaolinite and high-Fe chlorite.

chlorite. The presence of either or both phases can be determined with certainty. Several procedures have been proposed, but the easiest to use is to place an oriented aggregate in an atmosphere of formamide, much as you place samples with smectite in an ethylene glycol atmosphere, only it takes about two weeks or more to get full expansion to 10.4 Å. Halloysite expands much faster than kaolinite in an atmosphere of formamide and the procedure can be used to distinguish collapsed halloysite from kaolinite (Churchman et al., 1984). A more involved method that intercalates kaolinite with DMSO to give $d(001) = 11.2$ Å has been devised by Calvert (1984). Bohor and Triplehorn (1993) reviewed intercalation processes in relation to the dispersion of kaolinitic flint clays. Studies of samples before and after any of these treatments allow estimates of the diffraction contributions of chlorite, halloysite, kaolinite, and any mixed-layered clay minerals that produce possible interferences in the $12^\circ 2\theta$ region. More about halloysite in the section on *sepiolite*, *palygorskite*, and *halloysite*.

The relative intensities of the chlorite 00 l series can be used to determine the total heavy metal content of the mineral as well as the distribution of the heavy metals between the silicate and hydroxide octahedral sites. Heavy metals in chlorite usually consist of Co, Cr, Fe, Mn, and Ni. Of these, Fe is by far the most important. In our discussion, we assume that the only heavy metal present is Fe. Mg and Al are the light metals in chlorite octahedral sites (except for Li in the rare chlorite cookeite). Mg is assumed here because the

difference in scattering power between Mg and Al is negligible for our purposes. The distribution of Fe with respect to Mg in the two layers is called the *symmetry*, and if the symmetry is zero, then equal proportions of Fe and Mg exist in the two sites. The use of the $00l$ intensities for these determinations requires that correct conditions are maintained for sample-length-beam-slit relations and for sample thickness, as discussed in Chapter 9.

The procedure described next is modified from Brown and Brindley (1980). It allows the determination of the total Fe content of chlorite, designated Y , and a measure of the symmetry of Fe substitution, defined as D and equal to the number of Fe atoms in the octahedral sheet of the silicate layer minus the number of Fe atoms in the hydroxide sheet. Both Y and D are based on a chlorite formula that contains a total of six metal atoms in both sites, and whose formula can be represented by $(\text{Mg,Al})_{6-y}\text{Fe}_y(\text{Si,Al})_4\text{O}_{10}(\text{OH})_8$. The maximum and minimum values for D are 3 and -3, respectively, and Y varies between 0 and 6. Brindley's method uses several $00l$ reflections, but we recommend only the 002, 003, 004, and 005, partly for the sake of simplicity, but also to eliminate errors in the 001 intensity that are caused by sample-length problems and uncertainties in the Lorentz factor.

Table 7.1 shows the intensity ratios $I(003)/I(005)$ and corresponding values of D . It is easy to measure this intensity ratio and to estimate D because there are no interferences from common minerals on these two reflections. Brown and Brindley's values have been calculated under the assumption of random orientation of the chlorite crystallites in the powder; consequently, you do not want very highly oriented sample preparations here. Very high $00l$ intensities indicate preferred orientation, and when that occurs the safest procedure is to base your intensity measurements on an unoriented

Table 7.1. $I(003)/I(005)$ and the symmetry of Fe distribution D

D	$I(003)/I(005)$
3.0	0.242
2.5	0.43
2.0	0.68
1.5	1.09
1.0	1.67
0.5	2.54
0.0	3.83
-0.5	5.76
-1.0	8.74
-1.5	13.3
-2.0	21.2
-2.5	34.1
-3.0	54.1

Values from Brown and Brindley (1980).

powder that has been packed into the back or side-loaded into a cavity-type

specimen holder (see Chapter 6). Unfortunately, the odd-order reflections are weak and may not be detectable from randomly oriented powders unless high concentrations of chlorite are present.

The determination of Y , the total number of Fe atoms, may be a bit difficult to apply in practice if there are kaolinite or serpentine interferences on the chlorite 002 and 004 peaks; otherwise the procedure is straightforward. First, using the following equation (Brown and Brindley, 1980), correct the value of $I(003)$ for any asymmetry to give $I(003)'$. The equation is given with the relevant constants.

$$I(003)' = I(003) \frac{I(003) (114)^2}{(114 - 12.1D)^2} \quad (7.1)$$

A measure of Y is then obtained according to the values shown in Table 7.2.

The application of these methods can yield precise results if you pay attention to details, and if there are no interferences on the chlorite reflections. Figure 7.5 shows calculated patterns for chlorites with different amounts of total Fe. The numerical methods are definitive, but we believe that the images are still important to the student for quick evaluations and for building up the critical experience that leads to an intuitive appreciation of the compositions involved.

The diffraction patterns of Fig. 7.5 illustrate the effects of total Fe on the intensities of the chlorite 001, 002, 003, and 004 reflections. The examples treat 2, 1, and 0 Fe atoms in each of the two octahedral sites: the silicate (Sil) and hydroxide (Hyd) sheets. The D value (symmetry) is zero. The example shows nicely how the odd-order peaks weaken, with respect to the even-order reflections, as the concentration of symmetrically distributed Fe increases.

Figure 7.6 illustrates the effects of Fe symmetry in chlorites. All calculated traces depict compositions with 1 Fe per Si_4O_{10} . Examples are shown for the Fe sited in the interlayer hydroxide sheet, in the silicate layer, and evenly distributed between the two layers. The large effect of Fe

Table 7.2. Estimation of the number of Fe atoms in six octahedral sites (Y)

Y	$[I(002) + I(004)] / I(003)'$
0	2.38
1	3.54
2	5.0
3	6.7
4	8.6
5	10.8
6	13.4

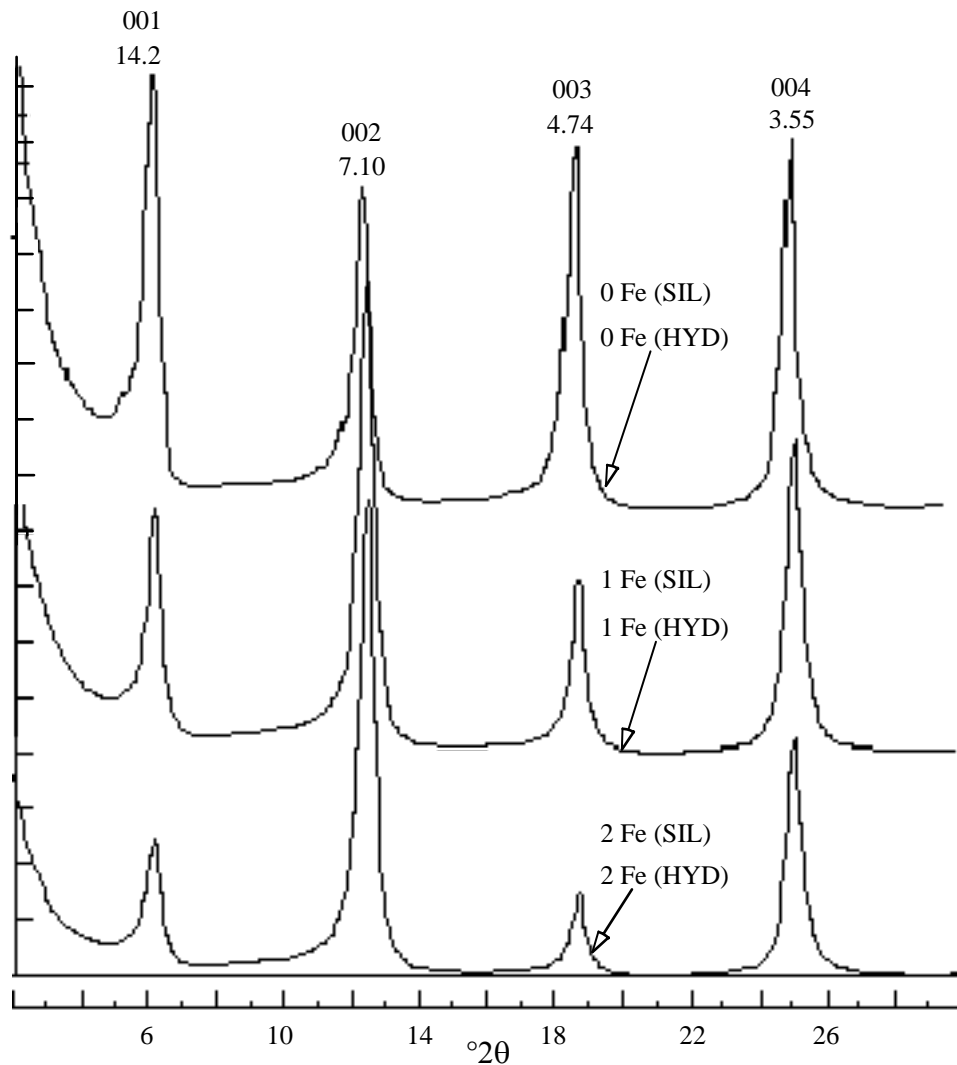


Fig. 7.5. Even/odd peak intensities in symmetrical chlorites as a function of Fe content. Numbers of Fe atoms refer to three octahedral sites per Si_4O_{10} .

symmetry on the intensity ratio of the 001 to 003 reflections is noteworthy. As a practical matter, you should remember that chlorites have symmetrical Fe substitution if their diffraction patterns show approximately equal intensities for the 001 and 003 peaks (Fig. 7.5).

The significant effect that Fe substitution has on diffracted intensity is due to the great difference in scattering power between Fe and Al or Mg (Chapter 3, p. 79). All this is perfectly consistent with the principles already outlined; still, it is nice to see the results in graphic form. Let us summarize the effects of Fe substitution in chlorite.

1. Increasing Fe or other heavy metal concentrations causes a weakening of the 001, 003, and 005 reflections relative to the 002 and 004 reflections.

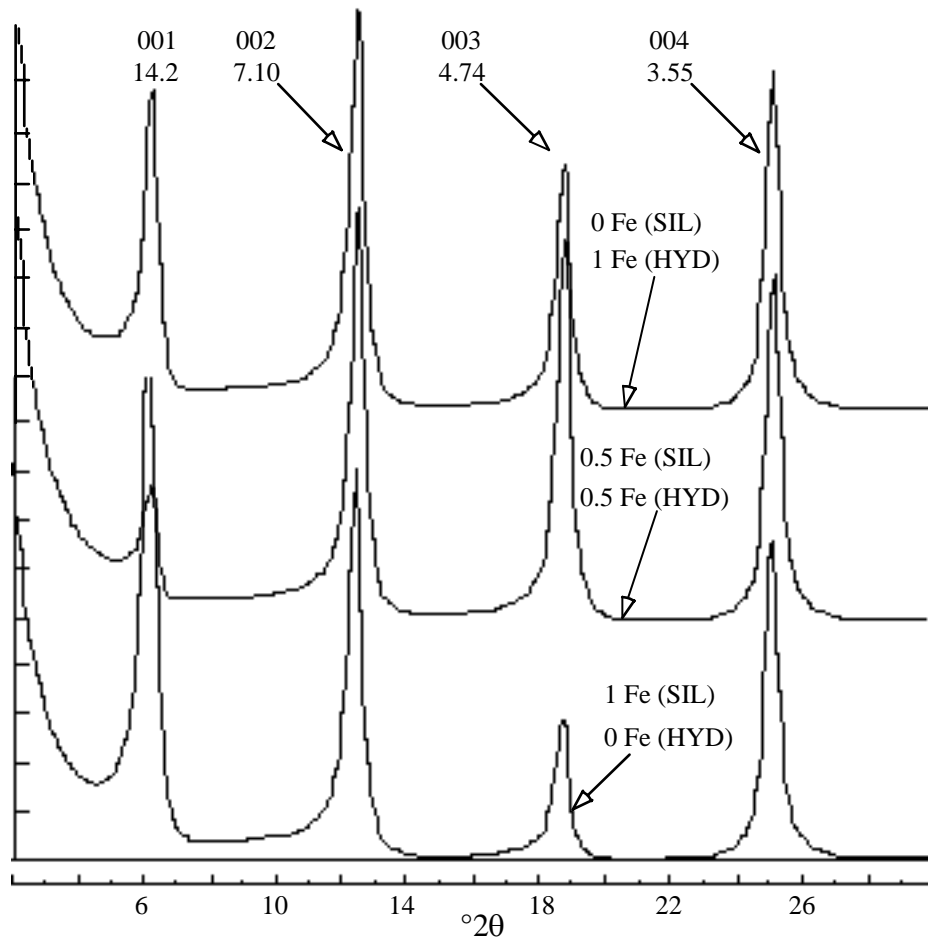


Fig. 7.6. Intensities of the 001 and 003 reflections of chlorites with identical total Fe contents, but with different values for Fe symmetry. Numbers of Fe atoms refer to each of the two octahedral sites that contain three atoms each.

2. Asymmetry of substitution that involves a relative enrichment of Fe in the silicate layer increases the intensities of the 001 and 005 reflections relative to the 003 reflections. For extreme cases, the diffraction patterns of such minerals resemble those of air-dried Mg-vermiculites.

3. Enrichment of Fe in the hydroxide sheet produces effects that are the reverse of those described in the second item. The 001 and 005 peaks are weak compared to the 003 reflection. This produces a strange-looking diffraction pattern that cannot be confused with that of any other clay mineral or mixture of clay minerals.

Vermiculite

Figure 7.7 shows the Mg-vermiculite diffraction pattern. It looks pretty much the same whether it is analyzed dry or after glycol solvation, assuming that it

is the Mg-saturated form that is common for most vermiculites. Na-saturated vermiculites give a strong peak in the $7^\circ 2\theta$ region, so if you are in doubt, Mg-saturate the sample and reanalyze it. The accepted definition of vermiculite is operational and requires that Mg-vermiculite retain a $d(001)$ of 14.5 \AA (like the one in Fig. 7.7) after *glycerol* (not ethylene glycol) solvation, whereas smectite produces a first-order peak at about 17.7 \AA ($5.0^\circ 2\theta$) after such treatment. Samples will be encountered that produce spacings intermediate between 14.5 and 17.7 \AA with glycerol and that collapse to 10 \AA after K saturation in the air-dried condition (Walker, 1958). These may be expandable clay minerals whose layer charges are intermediate between vermiculite and smectite, or they may be mixed-layered structures. At present, such minerals are poorly understood.

The vermiculite 001 reflection is intense, allowing the detection of very small amounts. Problems arise when small amounts of vermiculite are mixed with chlorite. The chlorite and vermiculite $00l$ reflections interfere, producing a pattern that looks like a chlorite with asymmetrical Fe substitution—in this case, a chlorite containing more Fe in the silicate layer than in the hydroxide sheet. The difficulty is easily resolved. K-saturate the sample or heat to 300°C

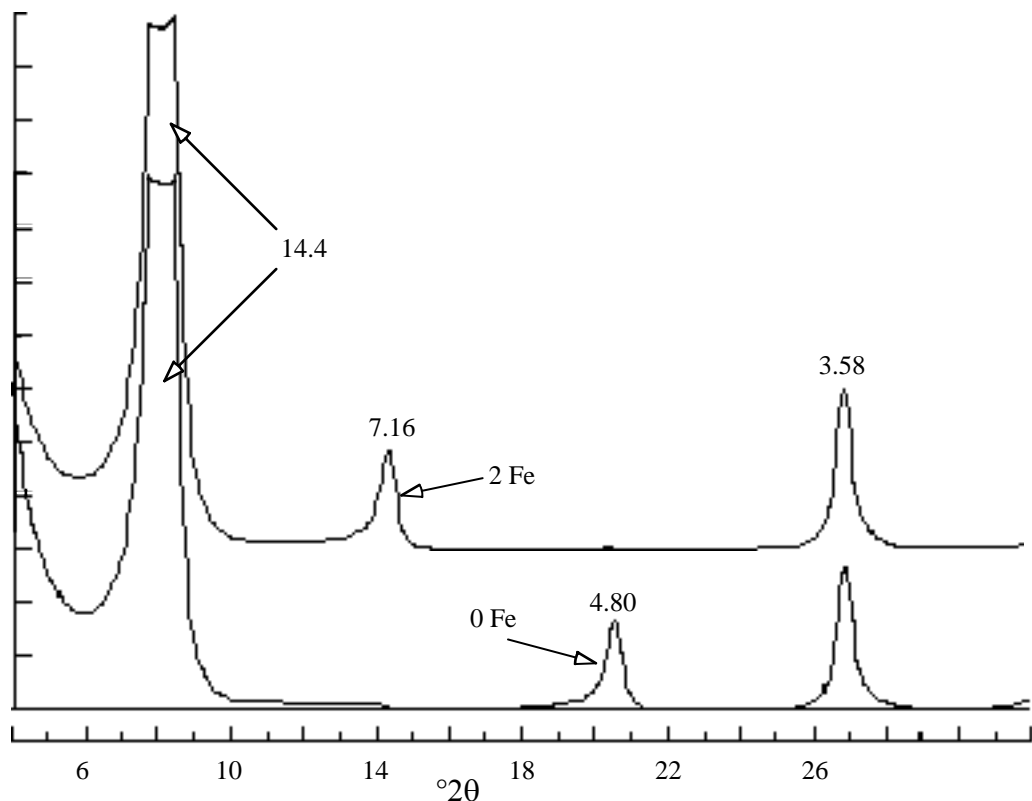


Fig. 7.7. Air-dried trioctahedral Mg-vermiculite. Fe values refer to three octahedral sites per Si_4O_{10} .

for an hour, and run a new diffraction pattern. These treatments collapse

vermiculite to 10 Å, remove the 00 l interferences, and change the vermiculite diffraction pattern to one similar to those of glauconite and biotite (the 002 reflection is very weak; see Fig. 7.3). Dioctahedral vermiculites can also be identified by these methods because the heat-treated mica-like pattern more closely resembles that of illite. The best procedure to distinguish trioctahedral from dioctahedral varieties is, however, to use the position of 060 reflection.

Figure 7.7 illustrates the effect of Fe for Mg substitution on the intensities of the vermiculite 00 l series. The intensity ratio of the 002/003 is a good measure of Fe content. Minerals that have 1 Fe per three sites show approximately equal intensities for these two reflections, and low-Fe dioctahedral varieties have diffraction patterns much like the 0 Fe composition of Fig. 7.7.

Smectite

Smectite is easily identified by comparing diffraction patterns of air-dried and ethylene glycol-solvated preparations. The glycol-treated preparation gives a very strong 001 reflection at about $5.2^\circ 2\theta$ (16.9 Å), which, in the air-dried condition, shifts to about 6° (15 Å) if the clay is saturated with a divalent ion and equilibrated with air at room temperature and moderate humidity. Confirmation of the identification, if necessary, is accomplished by K-saturation and drying at 300°C. This treatment collapses smectite to 10 Å, producing a diffraction pattern similar to that of illite.

The major difficulty in smectite identification lies in judging whether the mineral is mixed-layered with illite. Small amounts of illite interstratification show up as a shift in the 003 peak to higher diffraction angles. Unfortunately, all glycol-solvated smectites do not produce a $d(001)$ of 16.9 Å, and a thinner glycol spacing also displaces the 003 reflection (Ś rodoń , 1980). To establish the presence of a different glycol thickness, you will have to measure carefully the 00 l positions and test for a consistent $d(001)$ by means of Bragg's law. If the diffraction pattern is rational (see Chapter 8), peak displacement cannot be due to interstratification. The 002 and higher-order reflections are relatively weak and may not be detectable on the diffraction pattern unless the sample contains significant amounts of smectite. If the higher-order reflections are not detectable, some useful information can be obtained from the shape of the 001 reflection (ethylene glycol-solvated), which will be broad, with a high low-angle shoulder if interstratified illite is present. But we defer further discussion of such details to the section on mixed-layered clay minerals. Figure 7.8 shows diffraction patterns of a common smectite, montmorillonite, in the air-dried (two-water-layer) and ethylene glycol-solvated states. Note that, like vermiculite, the 001 is very intense, allowing detection of amounts as small as a few percent.

The smectite 00 l intensities, like those of chlorite, can be used to gain information on Fe substitution or, more accurately, on the scattering from the

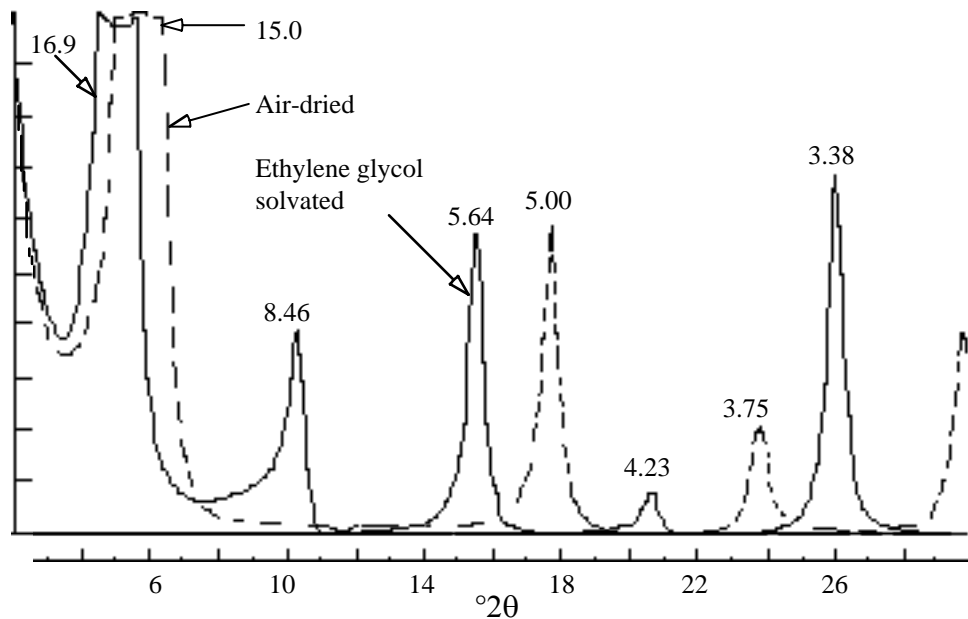


Fig. 7.8. Montmorillonite in the air-dried and ethylene glycol-solvated states.

octahedral sheet. Figure 7.9 shows patterns for three minerals with different amounts of Fe per two octahedral sites, montmorillonite with 0.1, Mg-saponite with none, and nontronite with 1.7. The intensity ratio of the 002 to the 003 increases sharply as the total number of electrons in the octahedral sites increases; this intensity ratio is useful for differentiating dioctahedral from trioctahedral smectites, though moderate Fe concentrations in a dioctahedral variety will produce diffraction patterns that are indistinguishable from Mg-rich trioctahedral varieties. The dilemma can be resolved by measuring the spacing of the 060, which differentiates dioctahedral from trioctahedral species provided that the sample does not contain other clay minerals that interfere with this reflection.

Montmorillonite can be distinguished from nontronite, saponite, and beidellite by its irreversible collapse after Li saturation and heat treatment. Speculation is that Li ions migrate into the octahedral sheet and neutralize the layer charge if the charge is due to octahedral substitution. The elimination of charge converts montmorillonite to a pyrophyllite-like mineral that does not expand upon treatment with water, glycerol, or ethylene glycol. The procedure is known as the Greene-Kelly test (Greene-Kelly, 1952, 1953). Modifications of the original procedure have been made that improve the performance of the test (Byström-Brusewitz, 1975), and they are included in the following description. Li-saturate a clay sample and remove excess LiCl reagent by multiple washings with water followed by silver nitrate tests to ascertain the absence of chloride. Mount the sample on an *opaque* fused silica slide (not glass or clear silica) and heat to 300°C for 12 h, saturate with *glycerol* and analyze immediately on the diffractometer. Rigid standardization

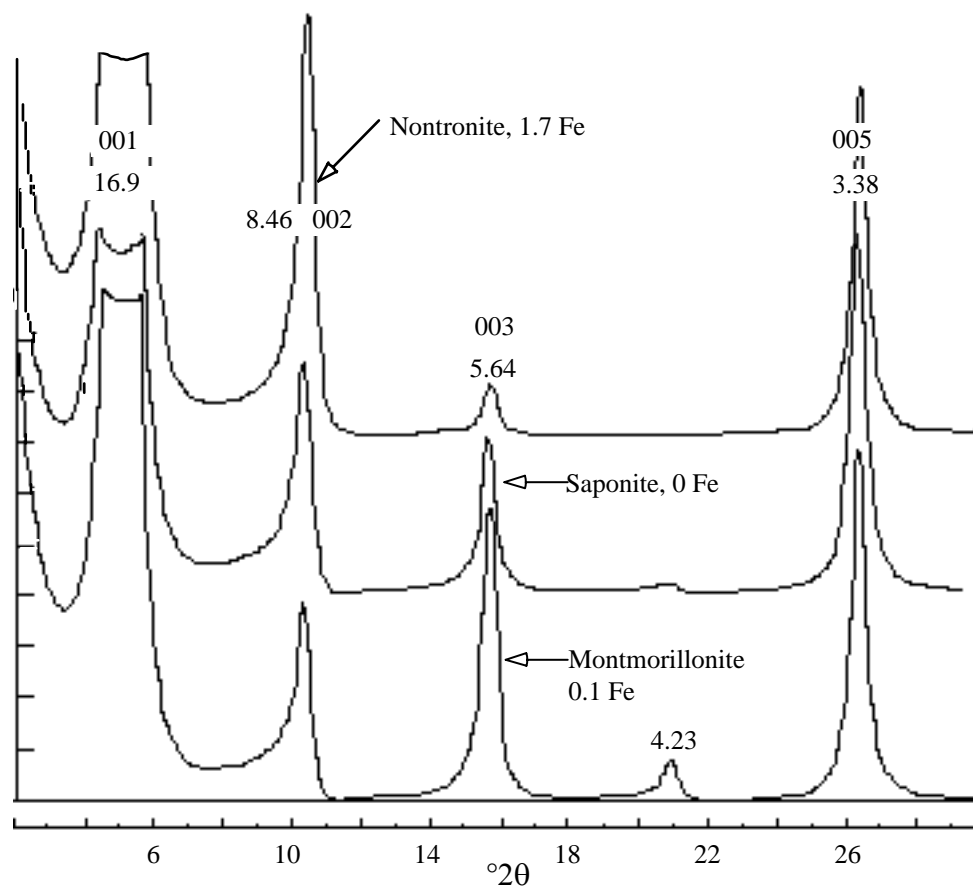


Fig. 7.9. Peak intensity as a function of octahedral scattering (Fe) in ethylene glycol-solvated smectites. Fe values refer to two or three octahedral sites per Si_4O_{10} .

of the procedures is essential for repeatable and significant results. We have found this method tricky to use, and ambiguous results can be obtained if attention is not paid to details.

After such treatment, montmorillonite is recognized by its collapsed state, which produces a first-order spacing of about 9.6 Å. The other smectites should expand to give the characteristic (glycerol-smectite) 17.7 Å reflection at 4.9 to 5.0° 2θ. Complex diffraction patterns may result, and if they do, the investigator will be hard pressed to classify them as evidence of interstratification, on the one hand, or failure of the treatment, on the other.

Sepiolite, Palygorskite, and Halloysite

Sepiolite, palygorskite, and halloysite are fibrous and cannot be oriented so that 00l reflections dominate the diffraction pattern. Instead, many lines from the *hkl* series are present, but because most lines are relatively weak they are difficult to detect unless the sample is rich in one of these minerals. Table 7.3 shows the relevant data for each, but bear in mind that a good deal of variation in spacings and intensities may occur from one sample to the next.

Table 7.3. X-ray data for sepiolite and palygorskite

Sepiolite			Palygorskite		
<i>d</i>	<i>I</i>	2 θ	<i>d</i>	<i>I</i>	2 θ
12.8	100	6.9*	10.4	100	8.5*
7.6	4	11.6	6.4	16	13.8*
5.1	8	17.4	5.4	11	16.4*
4.4	35	20.2	4.46	17	19.9
3.77	20b	23.6*	3.65	10	24.4*
3.35	30vb	26.6	3.18	16	28.1*

b = broad, vb = very broad

Reflections marked with an asterisk are common to several different specimens of these two minerals and are free from interferences by other minerals common in the clay-size fraction. The palygorskite data are a composite from Bailey (1980). The sepiolite values are taken from JCPDS powder diffraction card 29-1492.

The diffraction patterns are unaffected by mild heat treatment (< 200°C) and ethylene glycol solvation, and the minerals are most easily identified on the basis of the strong reflections at low 2 θ .

In most samples from sedimentary rocks, sepiolite and palygorskite will be minor constituents and only the low-angle peaks will be detectable—take care not to confuse them with mixed-layered clay minerals or vermiculite or smectite. These and other peaks are near the diffraction angles for many of the mixed-layered and expandable clay minerals. Additional sample treatments such as heating and ethylene glycol solvation may be necessary to differentiate mixed-layered and expandable species from either of these two minerals. In the older literature, sepiolite and palygorskite may have been misidentified as mixed-layered clay minerals, particularly as illite/chlorite.

Halloysite is a kaolin mineral whose habit is most commonly fibrous instead of platy. Crystals cannot be oriented in basal parallel fashion. The 00 l peaks are relatively weak, and nonbasal reflections are strong at about 20 and 35° 2 θ . The latter are asymmetrical with slowly diminishing intensity toward high diffraction angles. They are two-dimensional diffraction bands indicative of turbostratic stacking along Z and resemble similar reflections from smectites. The 00 l reflections are usually broader than those from kaolinite, though this criterion is by no means definitive. Dehydrated halloysite is a good guess for a mineral that gives broad, kaolinite-like 00 l and strong asymmetric hk reflections despite efforts to achieve good preferred orientation.

060 REFLECTIONS

X-ray diffraction studies of randomly oriented powders provide useful adjuncts to the identification of the clay minerals and to refinements in qualitative classification. The 060 reflections allow the distinction between

Table 7.4. Values of $d(060)$ and 2θ for micas and clay minerals

Mineral	$d(060)$	2θ
Kaolinite	1.490	62.31
Montmorillonite	1.492-1.504	62.22-61.67
Illite (Muscovite)	1.499	61.90
Glauconite	1.511	61.35
Saponite	1.520	60.95
Nontronite	1.521	60.91
Hectorite	1.530	60.51
Serpentines	1.531-1.538	60.47-60.16
Biotite	1.538	60.16
Chlorites	1.538-1.549	60.16-59.69
Sepiolite	1.540-1.550	60.07-59.65
Vermiculite	1.541	60.03
Berthierine	1.555	59.44
Palygorskite	1.56	59.23

All data are from Bailey (1980) except for the smectites, which are taken from Brindley (1980).

dioctahedral and trioctahedral types because the b cell dimension is sensitive to the size of the cations and to site occupancy in the octahedral sheet and is unaffected by the monoclinic angle β . The peaks are weak, but can be satisfactorily resolved from the background by step-scan procedures that use long count times or by chart recording at slow goniometer and chart speeds ($0.5^\circ/\text{min}$ and 0.5 cm/min), in conjunction with a long time constant (4 sec) and a small scale factor (1,000 cps full-scale). Table 7.4 shows nominal values of $d(060)$ and the corresponding diffraction angles.

The $d(060)$ values vary somewhat for a given mineral species because they depend on the composition of the octahedral sheet, the amount of Al in tetrahedral coordination, and the degree of tetrahedral tilt. Nevertheless, you can see that dioctahedral and trioctahedral types are clearly separable, with the exceptions of saponite and nontronite, which have nearly identical values for $d(060)$.

Be careful when identifying trioctahedral species because of the possible presence of a quartz peak at $d = 1.542\text{ \AA}$. If your sample contains quartz, look for another quartz reflection at $d = 1.82\text{ \AA}$. This reflection has about the same intensity as the peak at $d = 1.542\text{ \AA}$. If the peak at $d = 1.82\text{ \AA}$ is present, allow for the interference of quartz if you choose to interpret a peak in the 1.54 \AA region as evidence for a trioctahedral clay mineral in the sample.

THE USE OF *hkl* REFLECTIONS FOR THE DETERMINATION OF POLYTYPES

Determination of polytypes is a further level of refinement in qualitative analysis. You will need a thick random powder specimen (Chapter 6) and a diffractogram with high peak-to-background resolution. The problems always center around peak interferences. The various clay mineral *hkl* reflections interfere with each other (e.g., micas and chlorites), and severe interferences can be caused by quartz and feldspars. Polytype determinations have been made infrequently because only exceptional samples are sufficiently monomineralic to allow measurements of the required diffraction peaks or the techniques for isolating the mineral you are interested in are too time consuming and complex. The most frequent polytype determinations are made for the chlorites, illite, glauconite, and the kaolin group.

Any of the polytypes can be disordered to any degree from a few rotational or stacking faults whose effects can hardly be noticed in the diffraction patterns to disorder complete enough so that only the *00l* and the *hkl* reflections with $k = 3n$ are present. Disorder is best illustrated with calculated three-dimensional diffraction patterns that are selected to demonstrate the effects of different kinds of disorder present in different amounts. This discussion is deferred to Chapter 10. The diagnostic tables given here apply only to ordered species, except for the clay-size chlorites that almost invariably show only sharp *00l* and $k = 3n$ lines on powder diffraction patterns (Bailey, 1980).

Chlorite Polytypes

The chlorite polytypes that can be easily determined from random powder studies are *Ia*, *Ib* ($\beta=90^\circ$), *Ib* ($\beta=97^\circ$), and *IIIb*. Table 7.5 shows the most useful peaks for their identification.

Table 7.5. Diagnostic reflections for the determination of chlorite polytypes by random powder methods

Type <i>Ia</i>			Type <i>Ib</i> ($\beta=90^\circ$)			Type <i>Ib</i> ($\beta=97^\circ$)			Type <i>IIIb</i>		
d	I	2 θ	d	I	2 θ	d	I	2 θ	d	I	2 θ
2.65	30	33.8	2.69	20	33.3	2.68	25	33.4	2.66	15	33.7
2.59	15	34.6	2.65	15	33.8	2.60	15	34.5	2.59	60	34.6
2.39	60	37.6	2.51	100	35.8	2.55	5	35.2	2.55	50	35.2
2.27	10	39.7	2.34	10	38.5	2.47	70	36.4	2.45	50	36.7
2.07	5	43.7	2.15	40	42.0	2.40	5	37.5	2.39	50	37.6
2.01	30	45.1	1.96	5	46.3	2.30	5	39.2	2.26	40	39.9
						2.11	20	42.9	2.07	10	43.7
						2.01	10	45.1	2.01	60	45.1

From Bailey (1980).

Table 7.6. Diagnostic reflections for the determination of kaolin polytypes by random powder methods

Kaolinite			Dickite			Nacrite			Metahalloysite		
d	I	2 θ	d	I	2 θ	d	I	2 θ	d	I	2 θ
3.84	45	23.15	3.26	10	27.34	3.44*	40	25.9	4.45	100	20.0
3.12*	55	28.6	3.10	10	28.83	3.09*	30	28.9	2.57	40	34.9
2.75	35	32.56	2.94	10	30.43	2.93	10	30.54	2.22	5	40.6
2.34	90	38.47	2.80	10	32.02	2.41*	100	37.3	1.69	20	54.45
2.29	80	39.34	2.32	95	38.75	2.26*	10	39.9			
2.18	30	41.34	2.21	15	40.81	2.09*	20	43.3			
1.99*	50	45.6	1.97	40	45.97	1.92*	45	47.4			
1.84	40	49.57									

The asterisk indicates averages of two or more unresolved peaks. From Bailey (1980).

The Kaolin Polytypes

Table 7.6 shows data that have been selected to provide the most useful lines for the identification of the kaolin polytypes kaolinite, dickite, nacrite, and metahalloysite.

The Micas, Illite, and Glauconite

The mica-like clay minerals in sedimentary rocks provide examples of the *1M*, *3T*, and *2M₁* polytypes. The *1M* structure is found in two modifications characterized by different patterns of octahedral cation ordering, the *trans*-vacant or *tv* (centrosymmetric) and the *cis*-vacant or *cv* (noncentrosymmetric) varieties. Think of the *tv* types as the traditional ones and the *cv* as the new kid on the block who may actually turn out to be abundant now that Drits and his colleagues have shown us how to identify it (Drits et al., 1984; Drits and Tchoubar, 1990). These structures have been briefly discussed in Chapter 4.

All these polytypes have a pair of strong diagnostic peaks that lie on either

Table 7.7. Diagnostic reflections for the mica polytypes

<i>tv 1M</i>			<i>cv 1M</i>			<i>3T</i>			<i>2M₁</i>		
d	I	2 θ	d	I	2 θ	d	I	2 θ	d	I	2 θ
4.35	15	20.4	3.88	40	22.9	3.87	35	23.0	4.29	10	20.7
4.12	10	21.6	3.58	30	24.9	3.60	30	24.7	4.09	10	21.7
3.66	50	24.3	3.12	50	28.6	3.11	30	28.7	3.88	30	22.9
3.07	50	29.1	2.86	55	31.3	2.88	40	31.1	3.72	30	23.9
2.93	10	30.5	2.68	20	33.4	2.68	10	33.4	3.49	30	25.5
									3.20	30	27.9
									2.98	35	30.0
									2.86	30	31.3
									2.79	25	32.1

Data from Bailey (1980) except for the *cv IM* pattern, which was calculated from unit cell parameters and atomic coordinates given by Drits et al. (1984). side of the illite 003 peak. Techniques for enhancing these peaks are discussed in Chapter 6.

The data for the *cv IM* and *3T* structures are so much alike that it takes a good pattern to tell the difference. Some of the key reflections differ between the two by 0.15 to 0.2° 2θ, and these differences are the only way to distinguish them. To do this requires a high-resolution diffraction pattern from structures with little or no disorder. To date, only two ordered *cv IM* occurrences have been identified, so we must assume that at present we do know much about the relative abundances of these two structures. All references in the older literature to clay-size *3T* polytypes are suspect pending further study.

Problems with polytype identification are caused by interferences from the diffraction patterns of common nonclay minerals such as quartz and feldspars. These interferences can be overwhelming because the key three-dimensional polytype lines are weak unless (1) rather involved sample preparation methods are used (Chapter 6) to assure random orientation and (2) sufficiently long count times are used to produce good peak to background resolution—count times that cause typical diffraction runs to take 6 to 8 h. In addition, sedimentary rocks may contain a mixture of polytypes that probably represent diagenetic and detrital components.

For these reasons, few studies have been made of clay mineral polytypes in sedimentary rocks, compared to the voluminous literature on basal diffraction patterns. But don't be scared off. Modern instrumentation has improved and continues to improve in many ways that provide solutions to some of the experimental problems. Be willing to work a little harder and pay more attention to sample preparation and instrumental details. Settle for a small number of a samples per study that have been exhaustively characterized instead of a large diffuse database that has only statistical significance. Any field that is poorly investigated is a fruitful one for important and perhaps spectacular findings.

NONCLAY MINERALS

Clay minerals are seldom found as monomineralic material. Nonclay minerals are almost always present, often in amounts so small that only their most intense peaks can be seen. What follows is more of a tabulation than a discussion, but it provides a summary of the diffraction characteristics of the most common nonclay minerals in the clay-size fractions of sedimentary rocks. We have pared the list to diagnostic peaks with significant intensity within the 2θ range normally scanned for clay minerals. All *d* values have been rounded to two decimal places. The 2θ angles are listed to one decimal place if *d* in the sources is given to two decimal places; if *d* is given to three

places, 2θ is listed at two. You may need to go to the JCPDS powder diffraction file (abbreviated as PDF) or to other authoritative sources for confirmation of an identification made with these tables. Again, we urge you to make a collection of patterns of the purest examples of minerals you will deal with most often.

A few final comments. How many peaks are necessary to identify a mineral? A rule of thumb that has been around for a long time is that you need three peaks, assuming, of course, that none of them is coincident with reflections from another mineral known to be present. Is this statistically valid? We don't know. But don't try to sell a mineral identification on a single peak. Five or more would be nice. A specification of three seems to be about right. How good should the agreement be between a mineral's relative intensities from the card and from an experimental pattern? The agreement should be very good indeed if the mineral has no cleavage such as quartz, garnet, pyrite, etc.; fair agreement (20 to 30%?) if the mineral has a few good cleavage directions such as the carbonates and some sulfates, worse if there is one predominant cleavage such as in many of the feldspars, and very poor (off by maybe a factor of 10) if the mineral has a pronounced habit (fibrous) or one excellent cleavage direction such as we find in the micas and clay minerals. Minerals with relatively wide ranges of solid solution such as the feldspars and carbonates also have peaks whose positions vary. These comments assume that you have prepared an oriented aggregate for the study of the clay minerals. If a random powder mount is used, such as that described in Chapter 6, discrepancies between the intensities from experimental patterns and the cards can be reduced for all minerals to discrepancies of perhaps 10% or less, but only if the chemical composition of your experimental sample is identical to the one described by the cards. The different scattering powers of the different ions are a factor in controlling diffraction intensities. The worst effect is due to Fe, because it has many more electrons than any of the other common cations in silicates, and in most rock-forming sulfates and carbonates. Substitutions involving Al, Si, Mg, and Na have little effect on intensity; Ca for Mg or K for Na produce significant intensity changes, but nothing like the large effects of Fe substitution for Mg in dolomite.

Remember that these minerals produce sharper peaks than the clay minerals, and this distinction is an important diagnostic criterion.

Silica Minerals

Low, or α -quartz, is by far the most common of the silica minerals in sedimentary rocks. Most clay-sized fractions contain at least a trace of it, and, as discussed previously, its diffraction lines can be used as an internal standard for the accurate and precise measurement of d values. However, you should not see much more than a trace of quartz in the $< 2 \mu\text{m}$ fractions of most rocks, for if you do it usually indicates that something is wrong with the sample preparation procedures. Large amounts of quartz in the $< 2 \mu\text{m}$

fraction, for properly prepared samples, indicate the presence of either glacial rock flour or siliceous microfossil types, such as radiolarians and diatoms whose original skeletal material is usually opaline silica, especially in younger sedimentary rocks.

Varieties of opaline silica (which are transformed by diagenesis to quartz) form a diagenetic transformation series that starts with amorphous opal (opal A), progresses through opal CT to opal C, and ends with chert (low-quartz). For details on the diffraction characteristics of opaline silica, see Jones and Segnit (1971) and newer work described below.

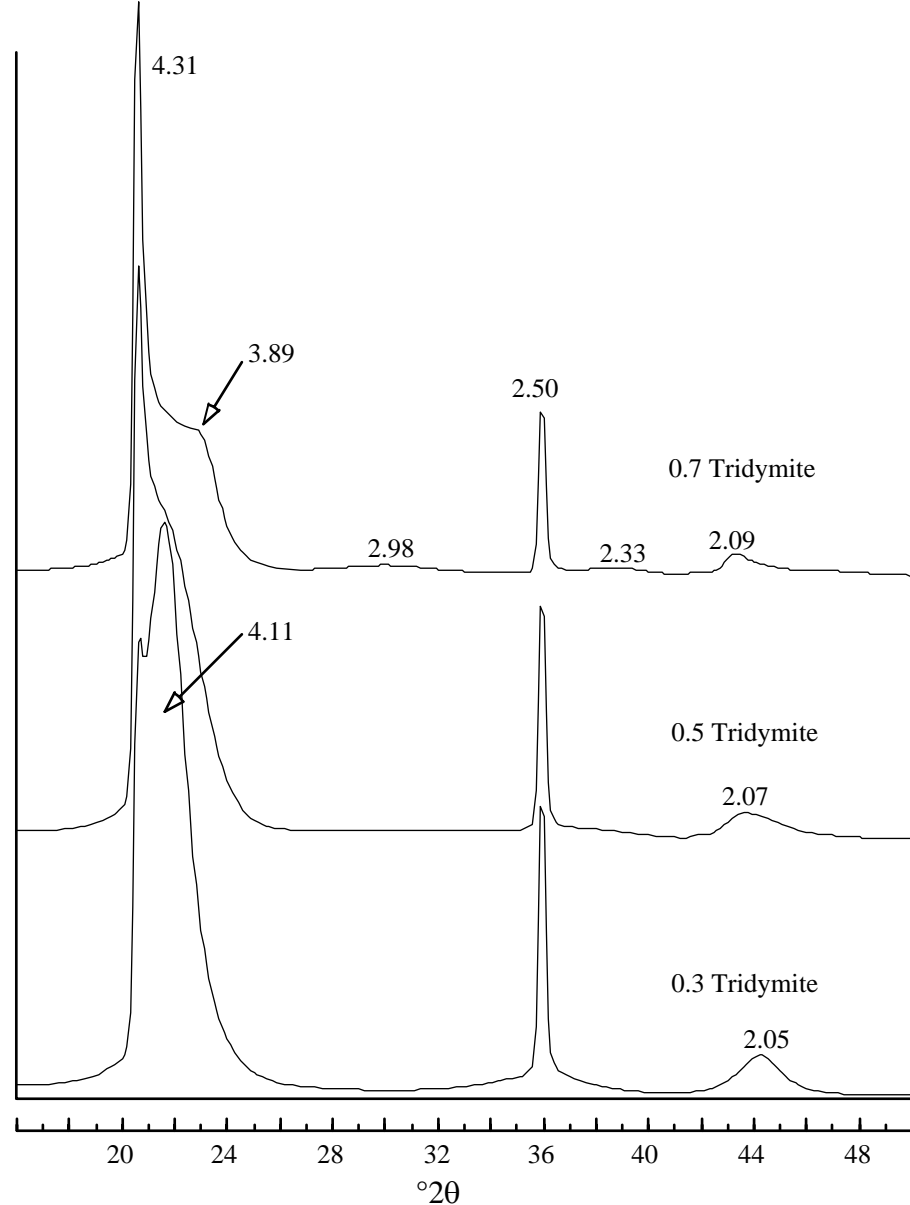


Fig. 7.10. Calculated diffraction patterns for randomly interstratified high-tridymite/high-cristobalite. See text for details.

Table 7.8A. Diffraction data for the silica minerals

Lo-Cristobalite ^a			Hi-Cristobalite ^b			Lo-Tridymite ^c			Hi-Tridymite ^d		
d	I	2θ	d	I	2θ	d	I	2θ	d	I	2θ
4.04	100	22.0	4.15	100	21.4	4.33	90	20.52	4.37	100	20.3
3.14	8	28.4	2.92	5	30.6	4.11	100	21.64	4.12	61	21.6
2.84	9	31.49	2.53	80	35.5	3.87	20	23.00	3.86	57	23.0
2.49	13	36.15	2.17	10	41.6	3.82	50	23.30	3.00	16	29.8
2.47	4	36.45	2.07	30	43.8	2.98	25	30.04	2.52	13	35.6
2.12	2	42.69	1.99	5	45.6	2.78	8	32.25	2.33	7	38.6
1.93	4	47.11	1.80	5	50.87	2.50	16	35.92	2.11	5	42.9
1.87	4	48.69	1.69	5	54.3	2.49	14	36.07			
			1.64	60	56.04	2.31	16	39.03			

^aPDF 39-1425. ^bPDF 4-359. ^cPDF 18-1170. ^dSee Brown (1980).

Figure 7.10 shows calculated three-dimensional diffraction patterns for randomly interstratified tridymite/cristobalite, or opal CT. These were computed by a version of WILDFIRE[®] modified in collaboration with G. D. Guthrie and D. L. Bish. Full details are given in Guthrie et al. (1995). The peak positions follow mixed-layered principles as described in Chapter 8. The high temperature structures of tridymite and cristobalite were used in the model structures, but if you compare these peak positions (Figure 7.10) with the pure end members (Table 7.8A) and allow for the effects of mixed-layering, you will see that the reflections on the calculated patterns are displaced somewhat toward higher diffraction angles. The best results for matches of experimental with calculated diffraction patterns required a reduction in the unit cell dimensions of the nominal silica layers that make up tridymite and cristobalite, and this alteration caused shifts of most reflections toward higher 2θ . The validity of this unit cell adjustment, with attendant shortening of Si-O bond lengths, and its possible significance is a subject that is still under study.

Estimates of the proportions of tridymite/cristobalite in opal CT are best made by (1) matching experimental/calculated diffraction profile shapes

Table 7.8B Diffraction data for α (low) quartz; from PDF Card 33-1161

d	I*	2θ	d	I	2θ
4.27	22	20.8	1.979	4	45.83
3.342	100	26.67	1.818	14	50.18
2.457	8	36.57	1.672	4	54.91
2.282	8	39.49	1.659	2	55.38
2.237	4	40.32	1.541	9	60.00
2.128	6	42.50	1.453	1	64.04

*These values replace those from PDF card 5-490, the data that were taken with a Geiger counter.

between 20 and $24^\circ 2\theta$, and (2) using the position of the peak near 44° .

Guthrie et al. (1995) report evidence of nearest neighbor ordering in some opal CT specimens, and this is manifested by a noticeable but unresolved peak on the high 2θ side of the strong reflection near $d = 4.11 \text{ \AA}$.

We offer a longer list of data for α -quartz because you will find it a useful internal standard everywhere but at low angles. Quartz d values are very constant from specimen to specimen, and its value as a standard justifies listing these spacings to more significant places than for the other minerals described here. The 1.54 \AA spacing, for example, is a standard against which the 060 of the clay minerals can be measured when you are distinguishing between dioctahedral and trioctahedral forms. A complete diffraction tracing and tabulation of spacings can be found in Frondel (1962, p. 34).

Feldspar

After you have established the presence of feldspar, you should ask, is it K-feldspar or plagioclase feldspar? Then, given good enough diffraction tracings, there may be a chance you can answer one or both of the following questions: What is the composition of the plagioclase? Is the K-feldspar triclinic or monoclinic or a mixture of the two? However, if you're going to get very involved with the feldspars, you had better change slit sizes to ones smaller than those you have been using for clay minerals and get ready for a career change. People have been wrestling with a reliable way to identify and measure the quantities of the varieties of feldspars for as long as there has been the recognition that the feldspars are a complex family of minerals. So, if you go much beyond the simple approximations offered here, expect to find disagreements and complications. For detailed information on feldspars see Ribbe (1983) or Smith and Brown (1988).

The low symmetry of feldspars means that they have complex diffraction patterns. Complicating the problem is that, unless they have been diagenetically homogenized, a variety of feldspars reflecting variation from source areas should be expected in sedimentary rocks. Almost as common as quartz in soils and fine-grained sedimentary rocks, they offer a confusing array of peaks. When trying to determine the polytype of illite, they are a bother. Table 7.9 consists of data selected from PDF cards 22-687, 19-926, 19-1227, 20-554, 9-466, 19-1184, 20-572, 10-393, 12-301, and 20-20, from Borg and Smith (1969a, 1969b), and from Herbert D. Glass, Illinois Geological Survey, Champaign, Illinois (personal communication, 1991). Both K-feldspar and plagioclase feldspars have variable compositions, and both are found as ordered and disordered varieties. In addition, many of the peak positions shift with composition changes. Therefore, we have rounded d off to the nearest 0.01 \AA and the 2θ positions to the nearest 0.05° . Several of the peaks represent diffraction from more than one hkl plane. If you need to know the hkl index of a plane, you will find it on the PDF cards listed above. The most intense peak for each of the four varieties of feldspars shown in Table 7.9 is underlined.

When looking at XRD traces from oriented aggregates, about the best you'll be able to do is to use the peak at $\sim 27.5^\circ 2\theta$ to indicate that some variety of K-feldspar is present, and the peak at $\sim 28^\circ 2\theta$ to indicate that some variety of plagioclase is present. For XRD traces of random powders, the peaks of the K-feldspars that are intense enough to show when feldspar is present in small amounts, that are not found in the plagioclase series, and that occur in the 2θ range normally used by clay mineralogists, are, in addition to the one mentioned above for oriented aggregates, two smaller ones at 21.10 and $25.65^\circ 2\theta$ for microcline, and 21.05 and $25.75^\circ 2\theta$ for orthoclase. The two peaks at the lowest angles can be useful only if they are resolved from the quartz peak at $20.8^\circ 2\theta$. You probably won't be able to distinguish microcline from orthoclase because 2θ positions vary with composition and degree of ordering. The most intense line of orthoclase and sanidine, which is at $26.75^\circ 2\theta$, is often of no use because it is interfered with by the strongest quartz line at $26.65^\circ 2\theta$. High sanidine-like feldspars as a diagenetic mineral are not uncommon in sedimentary rocks. When it is the only feldspar present, the peak at $27.5^\circ 2\theta$ is the most useful. But, when microcline is also present, the peaks at 29.7 and $30.7^\circ 2\theta$ are more useful because they are distinct from microcline peaks.

Two useful peaks in the plagioclase series not found in the alkali series, in addition to the $\sim 28^\circ 2\theta$ peak, are at 22.05 and $24.90^\circ 2\theta$. The peak at 23.50°

Table 7.9 Diffraction data for feldspars (2θ for $\text{CuK}\alpha$ radiation)

Microcline(Tr)		Ortho.(Mono)		Albite		Anorthite		Hi Sanidine	
d	2θ	d	2θ	d	2θ	d	2θ	d	2θ
4.22	21.06	4.22	21.05					4.24	20.95
				4.03	22.05	4.04	22.00		
3.80	23.40			3.68	24.90				
		3.47	25.66						
3.29		<u>3.31</u>	<u>26.75*</u>			<u>3.33</u>	<u>26.75</u>		
<u>3.24</u>	<u>27.52</u>	3.24	27.53			3.28	27.15		
								3.23	27.60
				<u>3.19</u>	<u>27.95</u>	<u>3.19</u>	<u>27.95</u>		
						<u>3.18</u>	<u>28.05</u>		
				3.15	28.25				
3.03	29.50	2.99	29.85					3.00	29.78
2.96	30.20			An ₃₃		An ₆₇			
				3.01	29.68	3.05	29.28		
2.89	30.95								
		2.77	32.35						

*The most intense peaks are underlined.

2θ is seldom useful because it is too close to peaks from the alkali series.

Under the best conditions you may be able to approximate the composition of the plagioclase by noting the position of the peak between 29.20 and $29.90^\circ 2\theta$. In a separate box in Table 7.9, the values for this peak are given for two specific values in the plagioclase series. Unfortunately, the variation in peak position does not vary regularly with composition. Under quite rare conditions you may be able to distinguish triclinic from monoclinic K-feldspar by comparing the microcline triplet at 29.50 , 30.20 , and $30.95^\circ 2\theta$, to that of orthoclase at 29.85 , 30.85 , and $32.35^\circ 2\theta$. At least two peaks are included in the table because they are so close to diagnostic peaks that you will probably not be able to resolve them. They are the anorthite peak at 28.05° , which should appear as a high-angle shoulder on the most intense peak for anorthite, and the microcline peak at 30.70° , which will probably be a bit more intense than the $30.95^\circ 2\theta$ peak.

The high-temperature, ordered, monoclinic K-feldspar sanidine is common in bentonites. Its pattern is similar to that of orthoclase. A useful way to infer the composition of the feldspars in the clay-size fraction is to study the silt fraction of a rock with a petrographic microscope or a microprobe.

There must be someone who loves feldspars, but to the clay mineralogist they are an unmitigated headache. They have many reflections that interfere with almost anything you want to do beyond simple qualitative analysis. Separation of very fine particle sizes ($<0.1 \mu\text{m}$ or less) seems to be the only way to get rid of them.

Zeolites

Zeolites are a surprisingly common constituent in clay-bearing rocks and they are frequently present in the clay-sized fraction. Table 7.10 gives the X-ray powder data for four of the most common minerals of this group. The data in Table 7.10 should be used with these important qualifications. Some zeolites are very susceptible to change under relatively gentle lab treatments. For example, heulandite will change structurally if it dehydrates, and it can dehydrate at $< 130^\circ\text{C}$. Clinoptilolite, classified by Breck (1974) as belonging to the same group as heulandite, is stable up to 700°C . A second qualification is that many zeolites are members of a solid-solution series. For example, analcime is the sodium-rich end of a series, the calcium-rich end of which is wairakite. In the structural position for a large cation, phillipsite can contain varying amounts of sodium, potassium, and calcium. With the variation in these, there are changes in the silicon-to-aluminum ratio in the tetrahedral sites. All this is to say that both peak positions and intensities should be expected to differ somewhat from the values in Table 7.10. Values for d and I in the table are rounded off from those in the original source, and only those peaks with an intensity of 10 or more are listed, except for the lowest-angle peaks for phillipsite and analcime. A strong clue for zeolites is the presence of

Table 7.10. Diffraction data for zeolites

Heulandite ^a	Clinoptilolite ^b	Phillipsite ^c	Analcime ^d
-------------------------	-----------------------------	--------------------------	-----------------------

d	I	2θ	d	I	2θ	d	I	2θ	d	I	2θ
8.96	100	9.9	8.95	13	9.9	8.11	8	10.9	9.14	2	9.7
7.94	12	11.1				7.18	63	12.3			
						7.16	66	12.4			
						6.42	17	13.8	5.60	60	15.8
5.26	10	16.8				5.38	19	16.5			
5.10	70	17.4				5.07	23	17.5	4.85	20	18.2
4.65	32	19.1	4.65	19	19.1	4.94	27	18.0			
3.98	65	22.3	3.98	61	22.3	4.13	36	21.5			
3.90	43	22.8	3.91	63	22.7	4.12	41	21.6			
3.84	11	23.2				4.06	18	21.9			
3.43	21	26.0							3.43	100	26.0
3.41	15	26.1				3.27	37	27.3			
3.18	19	28.1	3.17	16	28.2	3.21	100	27.8			
3.13	22	28.5	3.12	15	28.6	3.14	35	28.4			
3.07	12	29.1	3.00	18	29.8	3.13	34	28.5	2.93	50	30.5
2.99	29	29.9	2.97	47	31.0	2.93	15	30.5			
2.97	91	31.0	2.79	16	32.1	2.76	20	332.6	2.69	16	33.3
2.81	23	31.8				2.75	36	32.6			
2.73	20	32.8				2.70	16	32.1	2.51	14	35.8
						2.68	21	33.4	2.23	40	40.5

These data have changed substantially from the 1st edition. It isn't that the minerals have changed; resolution and detection have improved. ^aPDF 41-1357. ^b PDF 39-1383. ^cPDF 39-1375; see PDF 12-195 also. ^dPDF 19-1180; see PDF 41-1478 also.

sharp reflections in the clay mineral range, roughly the range below about 12° 2θ. Among the common minerals, only gypsum has a reflection there. For additional information on zeolites, see Mumpton (1977).

Carbonates

Carbonates, especially calcite and dolomite, are commonly associated with clay minerals. Peak positions will vary with the limited solid-solution series between calcite and dolomite and between ankerite and dolomite. They also will vary for the complete solid-solution series between siderite and magnesite and between siderite and rhodocrosite and for the limited substitution of Ca²⁺ for Fe²⁺ in siderite. Other carbonates that you could encounter in sedimentary rocks are smithsonite, rhodocrosite, and kutnahorite. The orthorhombic carbonates tend to have fewer ionic substitutions, therefore there is less variation in their peak positions. Strontianite and all the rhombohedral carbonates but magnesite form concretionary masses in shales. Vaterite, though it is unstable, is included here because it is produced by some immature forms of brachiopods and molluscs and may therefore be found in Recent sediments. X-ray data for eight carbonates are given in Tables 7.11A and 7.11B. Notice that, except for siderite, all of them have one very strong

Table 7.11A. Diffraction data for the rhombohedral carbonates

Calcite ^a			Ankerite ^b			Dolomite ^c			Siderite ^d		
d	I	2θ	d	I	2θ	d	I	2θ	d	I	2θ
3.86	12	23.0	2.91	100	30.72	2.89	100	30.98	3.59	25	24.78
3.04	100	29.43	2.20	5	41.04	2.67	4	33.56	2.80	100	32.02
2.50	14	36.00				2.41	7	37.39	2.35	20	38.37
2.29	18	39.43				2.19	19	41.18	2.13	20	42.35
2.10	16	43.18				2.02	10	44.99	1.96	20	46.42
			1.797	6	50.85	1.787	13	51.10			

^aPDF 5-586. ^bPDF 41-586 (the 3 most intense peaks!!). ^cPDF 36-426. ^dPDF 29-696.

Table 7.11B. Diffraction data for the orthorhombic carbonates plus vaterite

Aragonite ^a			Strontianite ^b			Witherite ^c			Vaterite ^d		
d	I	2θ	d	I	2θ	d	I	2θ	d	I	2θ
3.40	100	26.24	4.37	14	20.34	4.56	9	19.5	4.23	25	21.0
3.27	50	27.25	3.54	100	25.19	3.72	100	23.9	3.57	60	24.9
2.73	9	32.80	3.45	70	25.82	3.67	53	24.3	3.29	100	27.1
2.70	60	33.18	3.01	22	29.64	3.22	15	27.75	2.73	90	32.8
2.48	40	36.21	2.84	20	31.52	2.66	11	33.75	2.11	20	42.86
2.41	14	37.36	2.60	12	34.55	2.63	24	34.12	2.06	60	43.96
1.98	55	45.82	2.55	23	35.14	2.59	23	34.63			

^aPDF 41-1475; ^bPDF 5-418; ^cPDF 5-378; ^dPDF 33-268.

peak and not much else. This makes their identification uncertain unless they are abundant enough to produce detectable weak reflections. What if you have to know? Treat the sample with hot, 1N HCl, wash by centrifugation, and analyze again. If the peak is still there, it is not due to a carbonate. We recommend starting with Reeder (1983) for additional information on any carbonates you may encounter.

Apatite, Pyrite, and Jarosite

Table 7.12 gives diffraction data for apatite, pyrite, and jarosite. Considerable substitution in apatite causes variation in peak positions, so the values given are guidelines. The JCPDS publication *Selected Powder Diffraction Data for Minerals* (1974) gives 26 cards for 26 different apatites; the 1993 version list them only by varietal name. Shown in Table 7.12 are two carbonate apatites. Specimen A is a natural specimen and specimen B is synthetic. Pyrite, if present in detectable amounts, produces a relatively high background with older machines because the incident CuK α radiation is ideal for exciting fluorescent radiation from iron. However, most of the excess background can be eliminated by using a single-crystal monochromator (p.50). Jarosite,

Table 7.12. Diffraction data for two carbonate apatites, pyrite, and jarosite

Apatite A ^a			Apatite B ^b			Pyrite ^c			Jarosite ^d		
d	I	2θ	d	I	2θ	d	I	2θ	d	I	2θ
8.13	18	10.9	3.46	25	25.8	3.13	35	28.54	5.93	45	14.9
4.06	10	21.9	3.04	10	29.4	2.71	85	33.07	5.72	25	15.5
3.43	16	26.0	2.78	100	32.2	2.43	65	37.02	5.09	70	17.4
3.08	25	27.0	2.68	40	33.4	2.21	50	40.79	3.65	40	24.4
2.81	80	31.83	2.62	10	34.20	1.92	40	47.45	3.11	75	28.7
2.77	25	32.27	2.23	16	40.43	1.63	100	56.34	3.08	100	29.0
2.72	100	32.97							2.97	15	30.14
2.63	12	34.13							2.86	30	31.26

^aPDF 21-145. ^bPDF 19-272. ^cPDF 6-710. ^dPDF 22-827.

KFe₃(SO₄)₂(OH)₆, may be an unfamiliar name to you, but it is a very common, yellow, weathering product of black shales and mudstones, particularly those in the arid western United States. Some have confused it with the uranium mineral carnotite, which it resembles. It forms by the oxidation of pyrite, which produces sulfuric acid that attacks illite and K-feldspar, liberates K, and forms the compound indicated by the formula.

Gypsum, Anhydrite, Celestite, and Barite

Data for these minerals are shown in Table 7.13. Gypsum is the likely phase in surface outcrops, but anhydrite is frequently found in subsurface samples such as well cuttings and cores. Gypsum is easily identified by its strong peak at $d = 7.56 \text{ \AA}$. Anhydrite has a similarly diagnostic reflection from a 3.50 \AA spacing. If gypsum has been heated, even to 60°C (e.g., to dry it), bassanite, $\text{CaSO}_4 \cdot 1/2\text{H}_2\text{O}$, may form. Its most intense reflection is a 3.00 \AA spacing ($29.80^\circ 2\theta$) but it has a diagnostic peak at $d = 6.01 \text{ \AA}$ ($14.75^\circ 2\theta$). The peak positions for these minerals will not vary much because there isn't much solid solution in them.

Table 7.13. Diffraction data for sulfates

Anhydrite ^a			Gypsum ^b			Celestite ^c			Barite ^d		
d	I	2θ	d	I	2θ	d	I	2θ	d	I	2θ
3.88	5	22.9	7.61	45	11.7	4.23	11	21	4.40	16	20.2
3.50	100	25.46	4.28	90	20.8	3.77	35	23.6	4.34	30	20.47
2.85	29	31.40	3.07	30	29.1	3.43	30	25.95	3.90	50	22.81
2.47	7	36.33	2.87	100	31.2	3.30	98	27.06	3.77	12	23.58
2.33	20	38.68	2.68	50	33.5	3.18	59	28.09	3.58	30	24.89
2.21	20	40.87				2.97	100	30.07	3.45	100	25.86
						2.73	63	32.79	3.32	70	26.86
						2.67	49	33.51	3.10	95	28.77
									2.84	50	31.55

^aPDF 37-1496. ^bPDF 21-816. ^cPDF 5-593. ^dPDF 24-1035.

Lepidocrocite, Goethite, Gibbsite, and Anatase

Lepidocrocite, goethite, and gibbsite are common in soils and some non-marine sedimentary rocks. Anatase is frequently encountered in shales, sandstones, and bentonites. Except for anatase, these minerals can produce broad reflections that resemble those of the clay minerals. Such peaks make it difficult to pick exact peak positions. These minerals lose water on heating to form new minerals. Therefore, heat treatment may provide useful confirmation of identifications.

Lepidocrocite on heating to 230 to 280°C forms maghemite $\gamma\text{-Fe}_2\text{O}_3$; and to hematite upon further heating to 400 to 500°C. Goethite forms hematite ($\alpha\text{-Fe}_2\text{O}_3$), which gives broad peaks. Heating to 900°C yields well-crystallized hematite with sharp peaks. Gibbsite on heating to 150 to 200°C changes first to boehmite $\gamma\text{-AlO(OH)}$, and then to a compound that doesn't occur as a

Table 7.14. Diffraction data for lepidocrocite, goethite, gibbsite and anatase

Lepidocrocite ^a			Goethite ^b			Gibbsite ^c			Anatase ^d		
d	I	2 θ	d	I	2 θ	d	I	2 θ	d	I	2 θ
6.26	100	14.2	4.98	12	17.8	4.85	100	18.3	3.52	100	25.3
3.29	90	27.1	4.18	100	21.24	4.37	70	20.3	2.43	10	36.98
2.47	80	36.4	3.38	10	26.34	4.32	50	20.6	2.38	20	37.83
2.36	20	38.1	2.69	35	33.27	3.36	17	26.5	2.33	10	38.61
2.09	20	43.3	2.58	12	34.73	3.18	25	28.1	1.89	35	48.09
1.94	70	46.90	2.49	10	36.09	2.46	25	36.5			
			2.45	50	36.68	2.38	55	37.8			
			2.25	14	40.02	2.16	27	41.8			
						2.05	40	44.2	1.98	10	45.8

^aPDF 8-98. ^bPDF 29-713. ^cPDF 33-18. ^dPDF 21-1272.

Table 7.15. Diffraction data for lepidocrocite, goethite, and gibbsite after heat treatment^a

(Lepidocrocite) $\gamma\text{-Fe}_2\text{O}_3$ ^b			(Goethite) $\alpha\text{-Fe}_2\text{O}_3$ ^c			(Gibbsite) $\chi\text{-Al}_2\text{O}_3$ ^d		
d	I	2 θ	d	I	2 θ	d	I	2 θ
5.90	5	15.0	3.67	35	24.3	4.52	30	19.6
4.82	5	18.4	2.69	100	33.3	2.38	70	37.8
3.73	5	23.9	2.51	75	35.8	2.12	80	42.7
3.40	5	26.2	2.20	25	41.0	1.90	30	47.9
3.20	10	27.9	1.84	30	49.5			
2.95	30	30.3						
2.51	100	35.8						

^aAll data from Rooksby (1961). ^{b,c}Formed by heating for 1 h at 300°C. ^dFormed by

heating for 1 h at 300°C; results could be indeterminate. mineral so far as we know χ -Al₂O₃. Data for XRD tracings of the phases resulting from such treatments are given in Table 7.15. The results from heating will not produce spectacular XRD tracings; gibbsite may be indeterminate, but in any event the gibbsite pattern will be destroyed.

Almost certainly we have left out your favorite mineral, but those given should do as starters. Brown and Brindley (1980, pp. 348ff) have provided an extensive table that is helpful or even indispensable for preliminary identifications. Copy this table and glue it to the wall of your X-ray diffraction laboratory.

SUMMARY

Discrete clay minerals are best identified from diffraction tracings of oriented aggregates. They show a *rational* series of 00*l* peaks. Clay and nonclay minerals are frequently mixed. The peaks of the nonclay minerals are usually sharper and narrower than those of clay minerals. A collection of diffraction tracings of the common, discrete clay minerals is probably the most useful tool for identification.

REFERENCES

- Bailey, S. W. (1980) Structures of layer silicates: in Brindley, G. W., and Brown, G., editors, *Crystal Structures of Clay Minerals and Their X-Ray Identification*, Monograph 5, Mineralogical Society, London, pp. 1-123.
- Bohor, B. F., and Triplehorn, D. M. (1993) Tonsteins: Altered Volcanic-Ash Layers in Coal-Bearing Sequences: *Special Paper 285*, Geological Society of America, Boulder, Colorado, 44 pp.
- Borg, I. Y., and Smith, D. K. (1969a) Calculated X-ray powder patterns for silicate minerals: *Geol. Soc. Amer. Memoir 122*, 896 pp.
- Borg, I. Y., and Smith, D. K. (1969b) Calculated powder patterns. Part II. Six potassium feldspars and barium feldspar: *Amer. Minerol.* 54, 163-81.
- Breck, D. W. (1974) *Zeolite Molecular Sieves*: Wiley, New York, 771 pp.
- Brindley, G. W. (1980) Order-disorder in clay mineral structures: in Brindley, G. W., and Brown, G., editors, *Crystal Structures of Clay Minerals and Their X-Ray Identification*, Monograph 5, Mineralogical Society, London, pp. 125-95.
- Brown, G. (1980) Associated minerals: in Brindley, G. W., and Brown, G., editors, *Crystal Structures of Clay Minerals and Their X-Ray Identification*, Monograph 5, Mineralogical Society, London, pp. 361-410.
- Brown, G., and Brindley, G. W. (1980) X-ray diffraction procedures for clay mineral identification: in Brindley, G. W., and Brown, G., editors, *Crystal Structures of Clay Minerals and Their X-Ray Identification*, Monograph 5, Mineralogical Society, London, pp. 305-59.
- Byström-Brusewitz, A. M. (1975) Studies of the Li test to distinguish beidellite from montmorillonite: *Proceedings, Internat. Clay Conf.*, 1972, Mexico City, Applied Publishing, Wilmette, Ill., pp. 419-28.
- Calvert, C. S. (1984) Simplified, complete CsCl-hydrazine-dimethylsulfoxide intercalation of kaolinite: *Clays and Clay Minerals* 32, 125-30.
- Chen, P.-Y. (1977) Table of Key Lines in X-Ray Powder Diffraction Patterns of Minerals in Clays and Associated Rocks: *Occasional Paper 21*, Geological Survey of Indiana, Bloomington, Indiana, 67 pp.

- Churchman, G. J., Whitton, J. S., Claridge, G. G. C., and Theng, B. K. G. (1984) Intercalation method using formamide for differentiating halloysite from kaolinite: *Clays and Clay Minerals* **32**, 241-48.
- Drits, V. A., Plançon, B. A., Sakharov, B. A., Besson, G., Tsipursky, S. I., and Tchoubar, C. (1984) Diffraction effects calculated for structural models of K-saturated montmorillonite containing different types of defects: *Clay Minerals* **19**, 541-61.
- Drits, V. A., and Tchoubar, C. (1990) X-Ray Diffraction by Disordered Lamellar Structures: Springer-Verlag, New York, 371 pp.
- Fron del, C. (1962) *Silica Minerals*, Vol. III, *The System of Mineralogy*: Wiley, New York, 334 pp.
- Greene-Kelly, R. (1952) Irreversible dehydration in montmorillonite: *Clay Mineral Bull.* **1**, 221-27.
- Greene-Kelly, R. (1953) Irreversible dehydration in montmorillonite. Part II: *Clay Mineral Bull.* **2**, 52-6.
- Guthrie, G. D. Jr., Bish, D. L., and Reynolds, R. C., Jr. (1995) Modeling the X-ray diffraction pattern of opal: *Amer. Minerl.* **80**, 869-72.
- Jones, J. B., and Segnit, E. R. (1971) The nature of opal I. Nomenclature and constituent phases: *J. Geol. Soc. Australia* **18**, 57-68.
- JCPDS (1993) *Mineral Powder Diffraction File Databook*: Joint Committee on Powder Diffraction Standards, Swarthmore, Pa., 781 pp.
- MacEwan, D. M. C., and Wilson, M. J. (1980) Interlayer and intercalation complexes of clay minerals: in Brindley, G.W., and Brown, G., editors, *Crystal Structures of Clay Minerals and Their X-Ray Identification*, Monograph **5**, Mineralogical Society, London, pp. 197-248.
- Mumpton, F. A., ed. (1977) *Mineralogy and Geology of Natural Zeolites*: Short Course Notes, Vol. **4**, Mineralogical Society of America, Washington, D.C., 233 pp.
- Reeder, R. J., ed. (1983) *Carbonates: Mineralogy and Chemistry: Reviews in Mineralogy*, Vol. **11**, Mineralogical Society of America, Washington, D.C., 394 pp.
- Rooksby, H. P. (1961) Oxides and hydroxides of aluminum and iron: in Brown, G., ed., *The X-Ray Identification and Crystal Structures of Clay Minerals*: Mineralogical Society, London, pp. 354-92.
- Reynolds, R. C., Jr. (1985) *NEWMOD*® a Computer Program for the Calculation of One-Dimensional Diffraction Patterns of Mixed-Layered Clays: R. C. Reynolds, 8 Brook Rd., Hanover, NH, 03755.
- Reynolds, R. C., Jr. (1986) The Lorentz-polarization factor and preferred orientation in oriented clay aggregates: *Clays and Clay Minerals* **34**, 359-67.
- Š rodoň , J. (1980) Precise identification of illite/smectite interstratifications by X-ray powder diffraction: *Clays and Clay Minerals* **28**, 401-11.
- Walker, G. F. (1958) Reactions of expanding lattice minerals with glycerol and ethylene glycol: *Clay Miner. Bull.* **3**, 302-13.